催化学报
2012 Chinese Journal of Catalysis Vol. 33 No. 9

Article ID: 0253-9837(2012)09-1495-07 **DOI**: 10.1016/S1872-2067(11)60429-4 **Article:** 1495–1501

Photodegradation of Organic Dye by CoS_2 and Carbon(C_{60}, Graphene, CNT)/TiO_2 Composite Sensitizer

MENG Zeda, OH Wonchun*

Department of Advanced Materials Science & Engineering, Hanseo University, Chungnam 356-706, Korea

Abstract: CoS_2, CoS_2-C_{60}/TiO_2, CoS_2-CNT/TiO_2, and CoS_2-Graphene/TiO_2 were prepared. The TiO_2 products had the anatase phase structure and interesting surface compositions. X-ray diffraction patterns of the CoS_2-carbon/TiO_2 composites showed a single and clear anatase phase and the CoS_2 structure. Scanning electron microscopy characterization of the texture on the CoS_2-carbon/TiO_2 composites showed a homogenous composition. Energy-dispersive X-ray spectra for elemental identification showed the presence of C and Ti with strong Co and S peaks from the CoS_2-carbon/TiO_2 composites. The composites obtained were also characterized by transmission electron microscopy and UV-Vis spectroscopy. CoS_2-carbon/TiO_2 composites showed excellent photocatalytic activity for the degradation of methylene blue under visible light irradiation. This was attributed to both photocatalysis on the TiO_2 support and charge transfer by the carbon nanomaterial, and the introduction of CoS_2 to enhance transfer of photogenerated electrons.

Key words: fullerene; carbon nanotube; graphene; cobalt disulfide; titanium dioxide; visible light; methylene blue; photodegradation

CLC number: O643 **Document code:** A

Received 5 April 2012. Accepted 5 June 2012.

**Corresponding author. Tel: +82-41-660-1337; Fax: +82-41-688-3352; E-mail: wc_oh@hanseo.ac.kr*

This work was supported by the Research Foundation from Hanseo University in 2011.

English edition available online at Elsevier ScienceDirect (http://www.sciencedirect.com/science/journal/18722067).

TiO_2 is the most widely used photocatalyst for the decomposition of organic compounds in air and water using irradiation of UV light with wavelength shorter than that corresponding to its band gap energy. It has a relatively high photocatalytic activity, biological and chemical stability, low cost, non-toxic nature, and long-term stability. However, the photocatalytic activity of TiO_2 is limited to irradiation with wavelengths in the UV region because the band gap of anatase TiO_2 is 3.2 eV and it can only be excited by photons with wavelengths below 387 nm [1,2]. However, only 3%–5% of the solar spectrum falls in this UV range. This limits the efficient utilization of solar energy by TiO_2. Some other problems still remain to be solved in its application, such as the fast recombination of photogenerated electron-hole pairs. Therefore, improving its photocatalytic activity by the use of modifications is a popular topic in recent years [3–7].

There has been much interest in the electronic structure of the transition metal dichalcogenides. A considerable number of experimental and theoretical studies have been reported on the pyrites, MX_2, with M = Mn, Fe, Co, Ni and X_2 = As_2, S_2, or AsS [8,9]. The crystal field splitting, electron correlation, and intrinsic 3*d* band-width are all of about the same magnitude in these compounds. These compounds range from diamagnetic semiconductors (FeS_2) to semi-metals ($FeAs_2$) according to the electronic configuration of the transition metal ion, and all of them have high specular and low diffuse reflectance throughout the visible region. This gives rise to a large variation in their electrical, magnetic, and optical properties. For instance FeS_2 is a diamagnetic semiconductor, while CoS_2 is a low-spin ferromagnetic metal [10,11].

A conjugated material is a good candidate for improving the transport of photocarriers in the photocatalytic process by TiO_2 because it has unique properties in electron or hole transport [12–14]. Carbon-based materials, such as graphite, carbon nanotubes (CNTs), graphene sheets, and fullerene have been widely studied. Two-dimensional (2-D) graphene has emerged as a high potential material for its fascinating physical properties including quantum electronic transport, extremely high mobility, high elasticity, and electromechanical modulation. Fullerene can efficiently promote a rapid photo-induced charge separation and slow down charge recombination in the dark, and it has been used to improve the performances of solar cell and in medicinal chemistry [15–17]. In the charge transfer between fullerene clusters and titanium dioxide under visible light, fullerene can be reduced by one-electron transfer in colloidal TiO_2 suspensions and form C_{60} [18–20]. Multi-walled CNTs are obtained by using a suitable catalyst support [21,22].

In this work, CoS_2-carbon/TiO_2 photocatalysts were prepared that showed significantly enhanced photocatalytic

activity for the degradation of methylene blue (MB) under visible light irradiation. The enhancement of photoactivity was attributed to photosensitization by CoS_2 and enhanced interfacial charge separation between the carbon layers and TiO_2 particles

1 Experimental

1.1 Synthesis of CoS_2-carbon composites

Crystalline fullerene (C_{60}) powder of 99.9% purity from TCI (Tokyo Kasei Kogyo Co. Ltd., Japan) was used as the carbon matrix. Crystalline multi-walled CNTs (MWCNTs; diameter: 20 nm, length: 5 μm) powder of 95.9% purity from Carbon Nano-material Technology Co., Ltd., Korea, was used as one of the carbon nanomaterials. Graphene oxide which was prepared by the Hummers-Offeman method in our previous work [23–25] was used as another carbon nanomaterial. For the oxidization of the carbon materials, 3-chloroperoxybenzoic acid (TCPBA) was chosen as the oxidizing agent. This was purchased from Acros Organics, New Jersey, USA. The oxidized carbon nanomaterials (54 mg) were added to $CoCl_2$ (DaeJung Chemicals & Metal Co., Ltd., Korea) and $Na_2S_2O_3$ (95%, Duksan Pharmaceutical Co., Ltd., Korea) solutions. After stirring, the mixture was added into a 100 ml Teflon-lined autoclave and maintained at 423 K for 12 h. The solvent was evaporated and the CoS_2-carbon (Graphene, C_{60}, or CNT) powder was obtained after drying. The samples are denoted as CoS_2-G, CoS_2-C_{60}, and CoS_2-CNT, respectively.

1.2 Synthesis of CoS_2-carbon/TiO_2 composites

CoS_2-carbon/TiO_2 was prepared using undiluted TNB and the CoS_2-carbon composite. CoS_2-carbon powder (3.4 g) was ultrasonicated (750 W, Ultrasonic Ptocessor VCX 750, Korea) for 30 min, and then mixed with 3 ml titanium *n*-butoxide (TNB, reagent grade, Acros Organics, USA). The solution was homogenized under reflux at 343 K for 5 h while being stirred. After stirring, the solution was transformed into a CoS_2-carbon/TiO_2 gel. This was heated at 673 K to give the CoS_2-carbon/TiO_2 composite.

1.3 Characterization

X-ray diffraction (XRD, Shimadzu XD-D1, Japan) was used to identify the crystallinity of the composite with monochromatic high intensity Cu K_α radiation (λ = 0.15406 nm). Scanning electron microscopy (SEM, JSM-5600, JEOL, Japan) was used to observe the surface state and structure of the composites. Transmission electron microscopy (TEM, JEOL, JEM-2010, Japan) was used to determine the state and particle size of the composites. TEM at an acceleration voltage of 200 kV was used to investigate the number and the stacking state of the graphene layers in the various samples. TEM specimens were prepared by placing a few drops of sample solution on a carbon grid. The elemental mapping of desired regions of the composites was determined by an energy-dispersive X-ray (EDX) analyzer attached to the SEM. UV-Vis diffuse reflectance spectra were obtained using an UV-Vis spectrophotometer (Neosys-2000, Scinco Co. Ltd., Korea) using $BaSO_4$ as a reference at room temperature, and the spectra were converted from reflection to absorbance spectra by the Kubelka-Munk method.

1.4 Photocatalytic degradation of MB

Photocatalytic activity was evaluated by MB degradation in aqueous media under visible light irradiation. For the visible light irradiation, the reaction beaker was located axially and held in a visible lamp box (8 W, halogen lamp, KLD-08L/P/N, Korea). The luminous efficacy of the lamp was 80 lm/W, and the wavelength was 400–790 nm. The lamp was located at a distance of 100 mm from the aqueous solution in a dark box. The initial concentration of MB (Samchun Pure Chemical Co., Ltd., Korea) was set at 1×10^{-5} mol/L in all experiments. The amount of photocatalyst used was 1 mg/ml. The reactor was placed for 2 h in the dark box to allow the photocatalyst particles to adsorb dye molecules to equilibrium. After the adsorption, the visible light irradiation was restarted to let the degradation reaction proceed. To perform dye degradation, a glass reactor (diameter: 4 cm, height: 6 cm) was used, and the reactor was placed on the magnetic stirrer. The suspension was then irradiated with visible light for a set irradiation time. Visible light irradiation of the reactor was performed for 90 min. Samples were withdrawn regularly from the reactor, and dispersed powder particles were removed in a centrifuge. The clear transparent solution was analyzed by a UV-Vis spectrophotometer (Optizen POP, Mecasys Co., Ltd., Korea). The dye concentration in the solution was determined as a function of the irradiation time.

The used CoS_2-C_{60}/TiO_2 composite was immersed in ethanol for 6 h and rinsed with deionized water, and then dried at 353 K. After this, the cleaned CoS_2-C_{60}/TiO_2 composite was reused for removing dyes, and the recycle experiment was done several times.

2 Results and discussion

2.1 Elemental analysis of the composites

Figure 1 shows the EDX spectra of CoS_2, CoS_2-C_{60}/TiO_2,

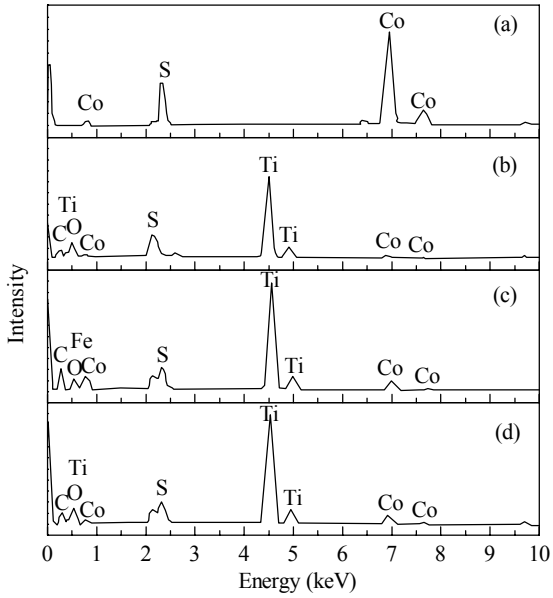

Fig. 1. EDX spectra of CoS_2 (a), CoS_2-C_{60}/TiO_2 (b), CoS_2-CNT/TiO_2 (c), and CoS_2-G/TiO_2 (d).

CoS_2-CNT/TiO_2, and CoS_2-G/TiO_2 compounds. The elemental composition of these samples was analyzed and the elements were identified using an EDX spectrometer. Figure 1 shows that strong K_α and K_β peaks from the Ti element appeared at 4.51 and 4.92 keV, respectively, while a moderately strong K_α peak for O was observed at 0.52 keV [26]. In addition to the above peaks, S and Co were also found. In Fig. 1, the quantitative microanalyses of C, O, Ti, Co, and S in the composites are shown. From the EDX data, the main elements were C, O, Ti, Co, and S. Table 1 lists the EDX quantitative microanalysis of the samples. In Fig. 1(c), the spectra showed the presence of C, O, and Ti as major elements, together with strong Co and S peaks. Some small impurities were observed, which were considered to have been introduced into the composites by using the fullerene without purification. In most samples, carbon and titanium

Table 1 EDX elemental microanalysis and BET surface areas of the photocatalysts

Sample	Elemental composition (wt%)						A_{BET}/
	C	O	Co	S	Ti	Impurity	(m^2/g)
C_{60}	99.99	—	—	—	—	—	85.05
CoS_2	—	—	54.71	44.09	—	1.20	20.95
CoS_2-C_{60}/TiO_2	22.30	34.02	11.09	1.27	31.18	0.13	43.58
CoS_2-CNT/TiO_2	20.02	37.32	10.71	1.32	30.17	0.46	49.35
CoS_2-G/TiO_2	21.81	38.74	7.33	1.96	29.97	0.19	52.67

.

were present as the major elements with small quantities of oxygen.

2.2 Surface characterization of the composites

Figure 2 shows the characterization of the surface structure and morphology of CoS_2, CoS_2-C_{60}/TiO_2, CoS_2-CNT/TiO_2, and CoS_2-G/TiO_2 compounds. In Figs. 2(a) and (b), the CoS_2 particles were subspheroidal particles and were well dispersed. Figures 2(c) and (d) show spherical C_{60} particles. C_{60} and CoS_2 were coated uniformly on the TiO_2 surface, which led to an increase in particle size. Zhang et al. [27] reported that well dispersed small particles provide more reactive sites for the reactants than aggregated particles. Figures 2(e) and (f) show that CNT and CoS_2 were coated uniformly and TiO_2 was supported on CNT and CoS_2 particles. Figures 2(g) and (h) show the lamellate graphene and subspheroidal CoS_2 particles clearly. There was more surface roughness when there was little grain aggregation. The aggregation became increasingly more, and TiO_2 addition caused more aggregation.

Table 1 lists the BET surface areas of the pristine C_{60}, CoS_2, CoS_2-C_{60}/TiO_2, CoS_2-CNT/TiO_2, and CoS_2-G/TiO_2 photocatalysts. The BET surface area decreased from 85.05 m^2/g for pure fullerene to 43.58 m^2/g for CoS_2-C_{60}/TiO_2. The TiO_2 and CoS_2 particles were deposited in the pores of fullerene, and the BET surface area value of CoS_2-C_{60}/TiO_2 decreased. The CoS_2-G/TiO_2 sample has a larger surface

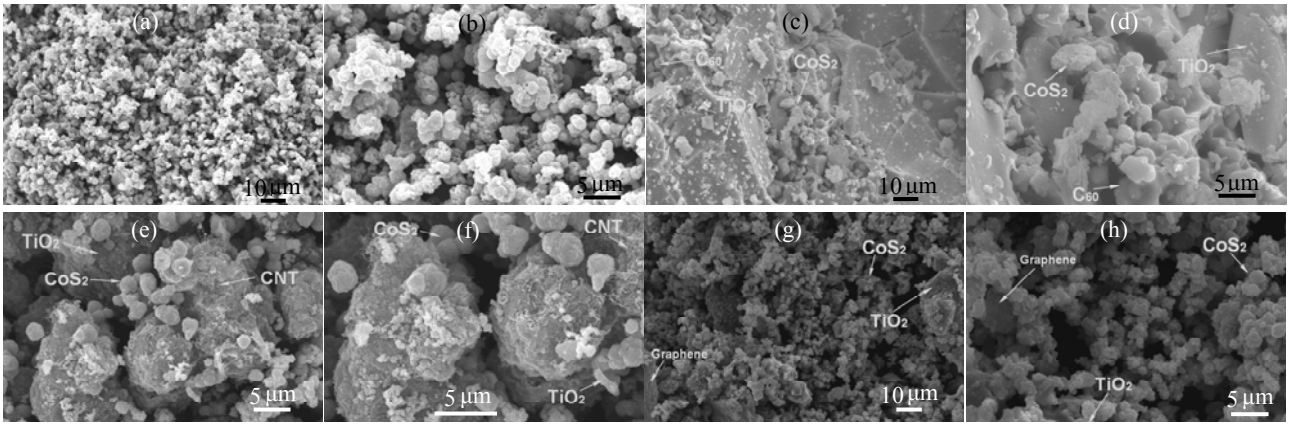

Fig. 2. SEM images of the samples. (a, b) CoS_2; (c, d) CoS_2-C_{60}/TiO_2; (e, f) CoS_2-CNT/TiO_2; (g, h) CoS_2-G/TiO_2.

area that can give more adsorption [28]. The carbon materials (C_{60}, CNT, and graphene) added can increase the surface area because these carbon materials have a relatively larger surface area. The BET surface area values for CoS_2 and the C_{60} modified CoS_2-TiO_2 compounds were 20.95 and 43.58 m^2/g, respectively. The BET surface area of the CoS_2 photocatalyst was increased when the particles were modified with the carbon materials. The CoS_2-G/TiO_2 photocatalyst has the largest BET surface area. This was because graphene has the largest pore size and pore volume. The pore size and pore volume were increased significantly when the particles were modified with the carbon materials because the carbon material particles have larger surface areas and pores.

Figure 3 shows the TEM images of CoS_2-C_{60}/TiO_2, CoS_2-CNT/TiO_2, and CoS_2-G/TiO_2 photocatalysts. The representative TEM images in Fig. 3 show that the powder particles were uniform with some aggregation of particles. From Fig. 3(a), the mean diameter of C_{60} was estimated to be 20 nm. Figure 3(b) shows that TiO_2 and CoS_2 particles were coated uniformly on CNT. Figure 3(c) is the TEM image of the CoS_2-G/TiO_2 photocatalyst, and it shows the lamellate graphene clearly. From Fig. 3, the images showed that all the particles had agglomerated. This suggested that the presence of CoS_2 and a carbon material can efficiently enhance the agglomeration of TiO_2 and impede the dispersion of the particles.

Figure 4 shows the XRD patterns of CoS_2, CoS_2-C_{60}/TiO_2, CoS_2-CNT/TiO_2, and CoS_2-G/TiO_2 composites. The XRD pattern of CoS_2 revealed a crystalline phase of CoS_2. The peaks at 2θ = 27.85º, 32.30º, 36.32º, 39.83º, 46.36º, and 54.97º were assigned to the (111), (200), (210), (211), (220) and (311) planes of the crystalline CoS_2 [29]. The XRD patterns of CoS_2-C_{60}/TiO_2 also showed C_{60} peaks at 2θ = 10.78º, 17.67º, and 20.75º, which were assigned to the (111), (220) and (311) planes of C_{60}. The XRD patterns also showed a crystalline phase of TiO_2. Peaks for CNT and graphene could not be found due to the presence of the small amount of CNT and graphene and the interference of

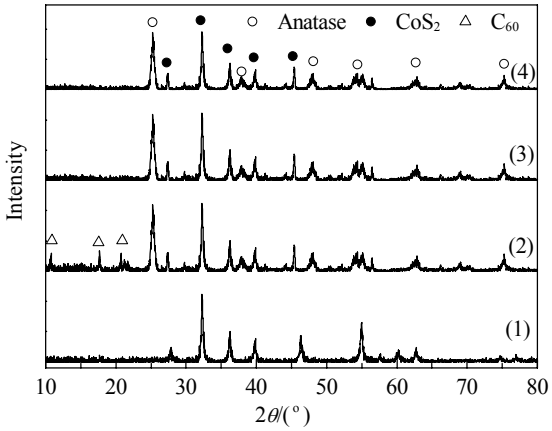

Fig. 4. XRD patterns of CoS_2 (1), CoS_2-C_{60}/TiO_2 (2), CoS_2-CNT/TiO_2 (3), and CoS_2-G/TiO_2 (4) photocatalysts.

TiO_2. The major peaks at 2θ = 25.3º, 37.5º, 48.0º, 53.8º, 54.9º, 62.5º, 68.7º, 70.3º, 75.1º, and 82.6º were assigned to the (101), (004), (200), (105), (211), (204), (116), (220), (215), and (224) planes of anatase, which showed that the TiO_2 was anatase [30].

2.3 UV-Vis diffuse reflectance spectroscopy

Figure 5 shows the UV-Vis absorption spectra of the samples. The UV-Vis absorption spectra for pure TiO_2, CoS_2, and CoS_2-C_{60}/TiO_2 composites showed strong absorption in the ultraviolet region. The absorption edge of TiO_2 was approximately 400 nm (E_g = 3.2 eV). In the visible region, the CoS_2 and CoS_2-C_{60}/TiO_2 composites showed good absorption, which indicated that these composites can have good photocatalytic activity under visible light irradiation. Since CoS_2 has a smaller band gap, it can be used to induce photocatalysis. When C_{60} was coupled with TiO_2, C_{60} acted as a photosensitizer, which can be excited to inject electrons into the conduction band of TiO_2. This suggested that the absorption in the visible region was due to the well dispersed C_{60} nanoparticles and not to any modification of the band gap of TiO_2 [31].

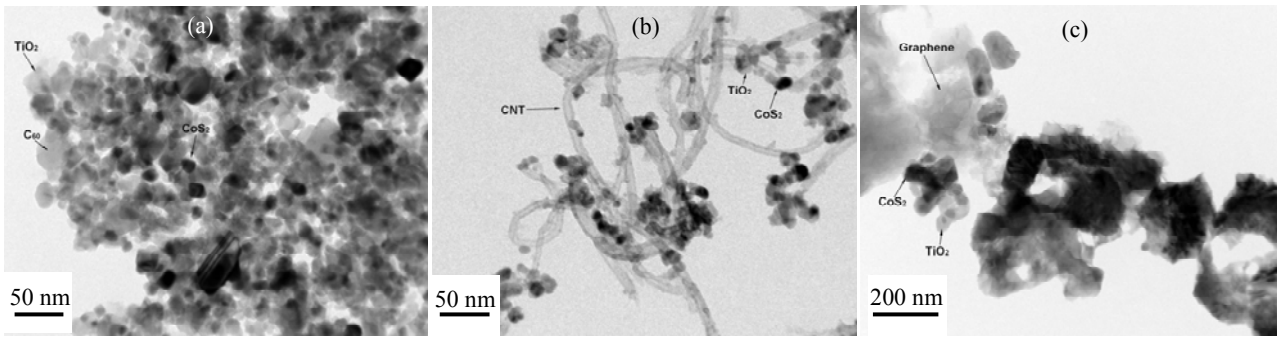

Fig. 3. TEM images of CoS_2-C_{60}/TiO_2 (a), CoS_2-CNT/TiO_2 (b), and CoS_2-G/TiO_2 (c) photocatalysts.

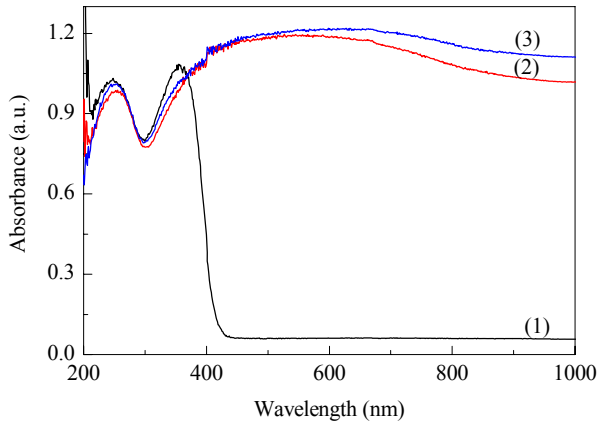

Fig. 5. UV-Vis absorption spectra of TiO_2 (1), CoS_2 (2), and CoS_2-C_{60}/TiO_2 (3) photocatalysts.

2.4 Photocatalytic activity of the composites

Figure 6 shows the changes with time during MB degradation using the CoS_2, CoS_2-C_{60}/TiO_2, CoS_2-CNT/TiO_2, and CoS_2-G/TiO_2 composites under visible light irradiation. The spectra for the MB solution after visible light irradiation showed the relative degradation yields at different irradiation times. The decrease in dye concentration continued, which was due to visible light irradiation. The concentration of MB was 1.0×10^{-5} mol/L, and the absorbance by MB decreased with increasing visible light irradiation time. The MB solution continuously lost its color, and the MB concentration continued to decrease. Two steps are involved in the photocatalytic decomposition of the dye: adsorption of dye molecule and its degradation. After adsorption in the dark for 2 h, the samples reached adsorption-desorption equilibrium. In the adsorption step, the CoS_2, CoS_2-C_{60}/TiO_2, CoS_2-CNT/TiO_2, and CoS_2-G/TiO_2 composites showed different adsorption amounts with CoS_2-G/TiO_2 giving the best adsorption (Fig. 6(a)). The adsorption of pure CoS_2 was the least. The adsorption by CoS_2-carbon/TiO_2 was better than that of CoS_2 because the added carbon materials enhanced the BET surface area, which increased the adsorption. CoS_2-G/TiO_2 has the largest BET surface area. In the degradation step, the CoS_2-C_{60}/TiO_2, CoS_2-CNT/TiO_2, and CoS_2-G/TiO_2 composites showed good degradation results. The CoS_2-C_{60}/TiO_2 composites showed good adsorption and degradation ability. A comparison of the decoloration by the catalysts showed that the degraded amount can be increased by an increase in the adsorption capacity. Figures 6(b) and (c) are the UV-Vis spectra of MB concentration for CoS_2 and CoS_2-C_{60}/TiO_2 composites as a function of time. As shown in the UV-Vis absorption spectra, the CoS_2-C_{60}/TiO_2 composites showed good adsorption and degradation result.

To evaluate the photochemical stability of the catalyst, the recycle experiments for the photodegradation of MB solutions were performed. The results are shown in Fig. 7. As shown in Fig. 7, 47% of MB was degraded when CoS_2-C_{60}/TiO_2 was used the first time. After four recycles, a small decrease of photocatalytic activity with CoS_2-C_{60}/TiO_2 was found, and 45% of MB was degraded in 90 min. In contrast, as shown in Fig. 7, the reused CoS_2-C_{60}/TiO_2 sample did not show a change in photocatalytic activity, which emphasized the excellent photochemical stability of the photocatalyst. This result is significant from the viewpoint of practical application as enhanced photocatalytic activity and prevention of catalyst deactivation gives a more cost-effective operation [32].

In the CoS_2-TiO_2 system, CoS_2 has a smaller band gap and can be used to induce photocatalysis by visible light irradiation. We propose that the hydroxyl radical on the surface of CoS_2 is easily transferred onto the surface of TiO_2. The organic pollutant adsorbed on the photocatalyst is

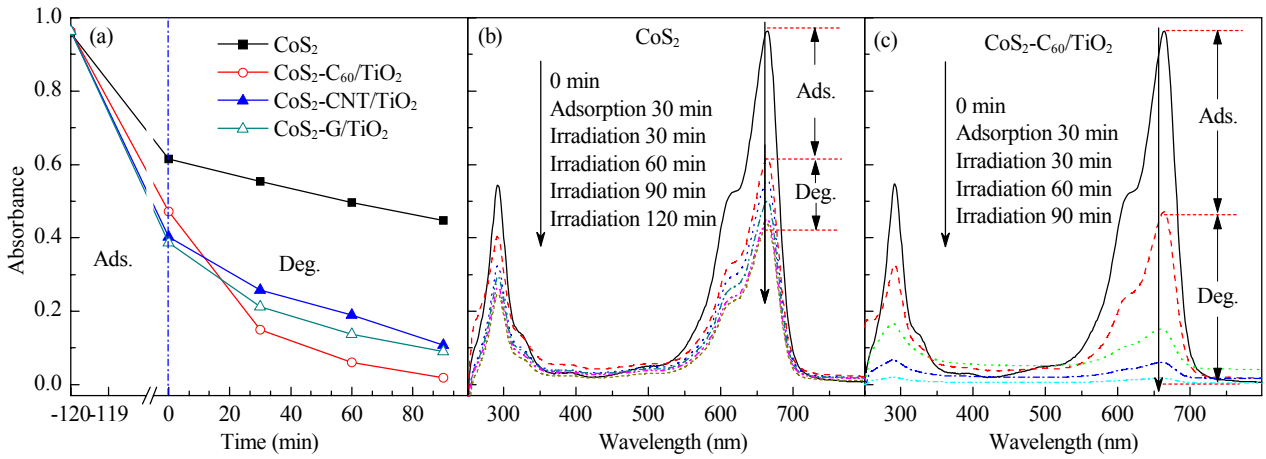

Fig. 6. Photocatalytic degradation of MB by different composites under visible light. Reaction conditions: visible light lamp 8 W, wavelength 400–790 nm, MB initial concentration 1×10^{-5} mol/L, catalyst 1 mg/ml. Ads.—adsorption; Deg. —degradation.

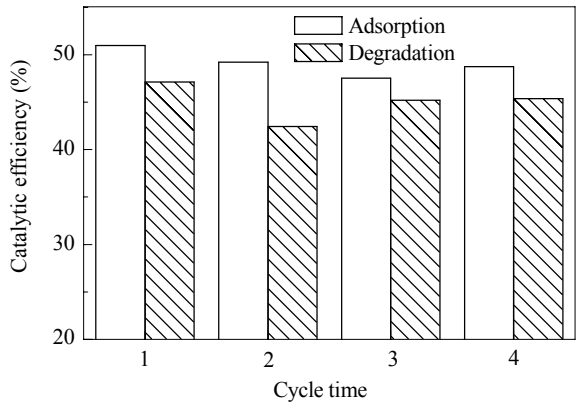

Fig. 7. Recycle experiments for CoS_2-C_{60}/TiO_2 composites.

degraded by the hydroxyl radical, resulting in the enhancement of the photodegradation performance of the sample [31]. CoS_2 acts as the energy sensitizer that improves quantum efficiency and increases charge transfer.

In the carbon material modified CoS_2-TiO_2 systems, MWCNTs and graphene act as electron sensitizers and donors in the composite photocatalysts, and can accept the electron (e^-) photo-induced by light irradiation. The electrons in CoS_2 can be transferred into the conduction band of the TiO_2 particles by MWCNTs and graphene. It is suggested that the photo-induced charge transfer occurred in the electronic interaction between the carbon layers or walls of the MWCNTs or graphene and the TiO_2. The electrons on the surface of MWCNTs and graphene migrate to the surface of the TiO_2 and this lead to less e^-/h^+ pair recombination and to an increase of the photon efficiency. These carbon materials can also enhance the adsorption during the discoloration process.

CoS_2-C_{60}/TiO_2 has a better degradation effect because fullerene is an energy sensitizer that improves the quantum efficiency and increases charge transfer, and at the same time, fullerene can enhance the adsorption during the discoloration process. When C_{60} is irradiated with visible light radiation, it is excited from the ground state to a short lived singlet excited state (ca. 1.2 ns), which undergoes rapid intersystem crossing at a rate of 5.0×10^8/s to a lower lying triplet state ($^3C_{60}^*$) with a long lifetime (> 40 μs). More important, photo-excited fullerenes are excellent electron acceptors capable of accepting as many as six electrons. $^3C_{60}^*$ has a higher electron accepting ability than ground state $^1C_{60}$, and electron-donating compounds can reduce $^3C_{60}^*$ to give the C_{60} radical anion ($^3C_{60}^-$). Electrons can be transferred from the conduction band of CoS_2 into the deposited $^3C_{60}^*$, resulting in the formation of $^3C_{60}^{\bullet-}$. This radical species would react with reactants adsorbed at the interface [26–29]. Thus, the deposition of C_{60} on the TiO_2 surface improves the photocatalytic activity. In addition, fullerene can generate e^-/h^+ pairs under visible light irradiation. It can be proposed that e^- transfer also happens between fullerene and TiO_2 in the composites, which retard e^-/h^+ recombination and increase photon efficiency. The light absorption capability of the photocatalyst and the separation of photo-generated e^-/h^+ pairs are crucial factors influencing the photo-activity. Oxidative degradation of azo dyes occurs by the attack of hydroxyl radicals and superoxide ions, which are highly reactive electrophilic oxidants. Due to the efficiency of hydroxyl radicals and superoxide ions, azo dyes were decompounded to CO_2, H_2O, and inorganic. Figure 8 shows a schematic diagram of the separation of photogenerated electrons and holes on the CoS_2-C_{60}/TiO_2 interface. Fullerene can efficiently promote a rapid photo-induced charge separation and slow down charge recombination. Fullerene can also efficiently promote generated e^-/h^+ pairs to enhance the degradation effect.

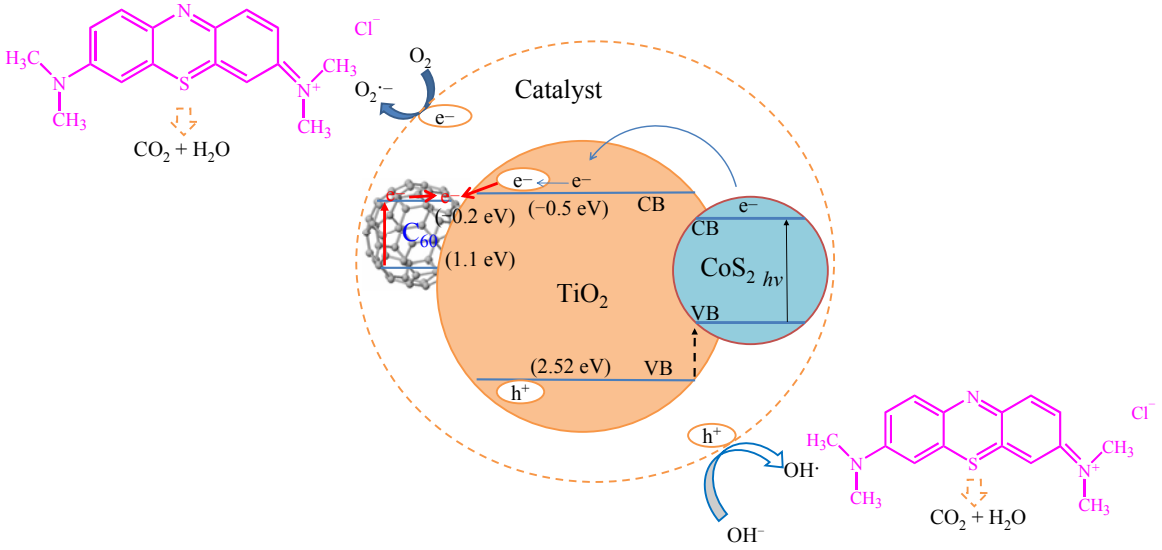

Fig. 8. Schematic of the separation of photogenerated electrons and holes on the photocatalyst interface.

3 Conclusions

Novel photocatalysts were successfully synthesized using a simple method. XRD patterns showed the cubic crystal structure of CoS_2. TEM showed that the surface of TiO_2 was coated uniformly with the carbon materials and CoS_2 layers. The diffuse reflectance spectra showed that the composites had strong absorption in the UV and visible range, and the presence of the carbon material enhanced the intensity of absorption in the visible range. The photocatalytic activity of the CoS_2-carbon/TiO_2 composites was examined by the degradation of MB in aqueous solutions under visible light irradiation. The CoS_2-C_{60}/TiO_2 composite showed good adsorption and degradation capacity.

References

1 Zhang F J, Chen M L, Zhang K, Oh W C. *Bull Korean Chem Soc*, 2010, **31**: 133
2 Oh W C. *J Photocatal Sci*, 2010, **1**: 29
3 Meng Z D, Zhang K, Oh W C. *J Korean Cryst Growth Cryst Technol*, 2009, **19**: 268
4 Yang Y, Li X J, Chen J J, Wang L Y. *J Photochem Photobiol A*, 2004, **163**: 517
5 Wu L, Yu J C, Wang X, Zhang L, Yu J. *J Solid State Chem*, 2005, **178**: 321
6 Saquib M, Muneer M. *Desalination*, 2003, **155**: 255
7 Xiang Q J, Yu J G, Jaroniec M. *J Phys Chem C*, 2011, **115**: 7355
8 Folkerts W, Sawatzky G A, Haas C, De Groot R A, Hillebrecht F U. *J Phys C*, 1987, **20**: 4135
9 Abrams B, Wilcoxon J. *Critical Rev Solid State Mater Sci*, 2005, **30**: 153
10 Bollinger M V, Jacobsen K W, Norskov J K. *Phys Rev B*, 2003, **67**: 085410
11 Scandella L, Schumacher A, Kruse N, Prins R, Meyer E, Luthi R, Howald L, Guntherodt H J. *Thin Solid Films*, 1994, **240**: 101
12 Chung H C, Huang Y C, Lee M H, Chang C C, Lin M F. *Phys E*, 2010, **42**: 711
13 Castro Neto A H, Guinea F, Peres N M R, Novoselov K S, Geim A K. *Rev Mod Phys*, 2009, **81**: 109
14 Wakabayashi K, Fujita M, Ajiki H, Sigrist M. *Phys Rev B*, 1999, **59**: 8271
15 Chang C P, Huang Y C, Lu C L, Ho J H, Li T S, Lin M F. *Carbon*, 2006, **44**: 508
16 Huang Y C, Chang C P, Lin M F. *Nanotechnology*, 2007, **18**: 495401
17 Lin M F, Shyu F L. *J Phys Soc Jpn*, 2000, **69**: 3529
18 Suzuki T, Kikuchi K, Oguri F, Nakao Y, Suzuki S, Achiba Y, Yamamoto K, Funasaka H, Takahashi T. *Tetrahedron*, 1996, **52**: 4973
19 Okazaki T, Lian Y F, Gu Z N, Suenaga K, Shinohara H. *Chem Phys Lett*, 2000, **320**: 435
20 Okazaki T, Suenaga K, Lian Y F, Gu Z N, Shinohara H. *J Chem Phys*, 2000, **113**: 9593
21 Jia J, Wang Y, Tanabe E, Shishido T, Takehira K. *Microporous Mesoporous Mater*, 2003, **57**: 283
22 Cassell A M, Raymakers J A, Kong J, Dai H. *J Phys Chem B*, 1999, **103**: 6484
23 Meng Z D, Zhu L, Choi J G, Chen M L, Oh W C. *J Mater Chem*, 2011, **21**: 7596
24 Oh W C, Chen M L, Cho K Y, Kim C K, Meng Z D, Zhu L. *Chin J Catal*, 2011, **32**: 1577
25 Zhu L, Meng Z D, Oh W C. *Chin J Catal*, 2011, **32**: 926
26 Meng Z D, Zhu L, Choi J G, Park C Y, Oh W C. *Nanoscale Res Lett*, 2011, **6**: 459
27 Zhang X W, Zhou M H, Lei L C. *Carbon*, 2005, **43**: 1700
28 Oh W C, Zhang F J, Chen M L. *J Ind Eng Chem*, 2010, **16**: 299
29 Li Y Q, Chen J H, Chen Y, Guo J. *Trans Nonferrous Met Chin*, 2011, **21**: 1887
30 Meng Z D, Peng M M, Zhu L, Oh W C, Zhang F J. *Appl Catal B*, 2012, **113-114**: 141
31 Apostolopoulou V, Vakros J, Kordulis C, Lycourghiotis A. *Colloid Surf A*, 2009, **349**: 189
32 Stylidi M, Kondarides D I, Verykios X E. *Appl Catal B*, 2004, **47**: 189